Research Square

Preprints are preliminary reports that have not undergone peer review.
They should not be considered conclusive, used to inform clinical practice,
or referenced by the media as validated information.

Performance Analysis of RIS Assisted D2D communications

Abdelkarim CHINBOU
Université Ibn-Tofail
Adil BOUMAALIF
adil.boumaalif@gmail.com

Université Ibn-Tofail
Ouadoudi ZYTOUNE
Université Ibn-Tofail

Research Article

Keywords: D2D communication, RIS, RIS Phase error, Transmit power distribution, Transmit power expectation, Transmit power optimization, RIS configuration selection

Posted Date: August 14th, 2025

DOI: https://doi.org/10.21203/rs.3.rs-7156655/v1

License: This work is licensed under a Creative Commons Attribution 4.0 International License.
Read Full License

Additional Declarations: No competing interests reported.

Performance Analysis of RIS Assisted D2D communications

Abdelkarim CHINBOU, Adil BOUMAALIF, Ouadoudi ZYTOUNE
Advanced Systems Engineering lab. (ASELab), Ibn Tofail University, University Campus, Kenitra, 14000, Morocco

***Abstract*—Reconfigurable Intelligent Surfaces(RIS) are emerging technologies to enable enhancing spectral and energy efficiency in the context of wireless communications. Device to Device (D2D) communication allows devices to communicate directly with each other, bypassing traditional base stations and reducing latency and congestion. Combined, RIS and D2D can significantly boost network performance, facilitate ultra-reliable low-latency communications, and contribute to more efficient and scalable wireless networks. Generally, RIS systems are composed of large number of elements and have a discrete phases shifting. Since RIS have limited signal processing capabilities, control messages are provided by a remote control center. Even if RIS can contribute to energy efficiency, this overhead impacts the transmission rate. In this paper we consider the case of D2D communications in the presence of a cellular interferer. We analyze the effect of RIS number of elements and phase resolution on the D2D transmit power. We derive the expectation of the transmit power, then we propose an iterative algorithm to optimize the transmit power by selecting the RIS configuration. Through extensive numerical simulation, we found that the obtained results prove the effectiveness of our analytic analysis.**

***Index Terms*—D2D communication, RIS, RIS Phase error; Transmit power distribution; Transmit power expectation; Transmit power optimization; RIS configuration selection.**

I. Introduction

THE unprecedented growth in wireless communication demands has pushed researchers and industry stakeholders to explore innovative technologies for beyond 5G and 6G networks. Among these emerging technologies, Reconfigurable Intelligent Surfaces (RIS), also known as Intelligent Reflecting Surfaces (IRS), have emerged as a promising solution to enhance wireless communication systems' spectral and energy efficiency [1]. These metasurface-based structures represent a paradigm shift in wireless network design, offering a sustainable and cost-effective approach to manipulating electromagnetic waves in propagation environments [2].

Traditional wireless communication systems rely heavily on active components such as amplifiers, mixers, and filters, which contribute significantly to the overall energy consumption and system complexity. In contrast, RIS technology introduces a nearly passive architecture comprising arrays of sub-wavelength metallic or dielectric elements that can be electronically controlled to modify the wireless propagation environment [3]. By intelligently adjusting the phase shifts of these elements, RIS can enhance signal coverage, mitigate interference, and improve the quality of service (QoS) for users in challenging propagation environments [4].

The integration of RIS in wireless networks aligns with the growing emphasis on green communications and sustainable technological solutions. As wireless networks continue to densify and energy consumption becomes a critical concern, RIS offers a promising alternative to traditional network densification strategies [5]. Unlike conventional relay systems that require active power-hungry components for signal processing and retransmission [6], RIS operates with minimal power consumption, primarily needed only for element reconfiguration and control signaling [7].

Moreover, the advent of RIS coincides with the evolution towards intelligent and programmable wireless environments, where network elements can adapt dynamically to changing channel conditions and user requirements. This technological convergence has sparked significant interest in both academia and industry, leading to numerous research initiatives and standardization efforts focused on RIS implementation and optimization [8].

The potential applications of RIS extend beyond traditional communication scenarios, encompassing diverse use cases such as millimeter-wave (mmWave) and terahertz (THz) communications, massive MIMO systems, non-terrestrial networks, and Internet of Things (IoT) deployments [9], [10], [11]. The versatility of RIS technology, coupled with its energy efficiency and cost-effectiveness, positions it as a key enabler for future wireless networks [12].

The operating principle of RIS is based on the concept of electromagnetic metasurfaces, which are artificially engineered structures composed of sub-wavelength scattering elements. Unlike traditional passive reflectors or relays, RIS offers unprecedented control over electromagnetic wave propagation through real-time reconfiguration of its elements. Each element typically consists of varactor diodes, PIN diodes, or other tunable components that can modify their electromagnetic properties in response to external control signals. The key capabilities of RIS include:

- Beamforming and Beam Steering: RIS can create highly directional beams and steer them towards desired users, maximizing signal strength at intended receivers while minimizing interference to others [8] [13].
- Non-Line-of-Sight (NLOS) Coverage Enhancement: By creating intelligent reflecting paths, RIS can extend coverage to shadowed areas and improve signal quality in NLOS scenarios [14] [15].
- Interference Suppression: Through careful phase configuration, RIS can destructively combine unwanted signals, effectively mitigating interference in multi-user scenarios [1] [13].
- Energy Efficiency: Unlike active relays, RIS operates without RF chains or signal processing units, offering

significant energy savings while maintaining performance benefits [13].

Phase error in Reconfigurable Intelligent Surfaces (RIS) arises due to discrete phase quantization and hardware imperfections that prevent precise phase adjustments, leading to degraded system performance. Unlike an ideal RIS that can continuously manipulate the phase of reflected signals, practical RIS implementations are constrained to a finite number of phase shifts [1] [2] [16] [17], typically L levels, where L = 2, 4, 8, etc. This quantization introduces phase noise, which disrupts constructive signal alignment, increases the bit error rate (BER), and reduces diversity gain. Studies have shown that for 1-bit phase quantization (L = 2), the diversity order is limited to $N/2$, while for $L \geq 3$, full diversity $G_d = N$ is achieved [18]. Furthermore, research suggests that higher phase quantization levels mitigate performance loss, and asymptotic BER analysis confirms that the impact of phase noise diminishes as quantization levels increase [19]. To address phase errors, recent advances propose adaptive phase shift optimization and deep learning-based RIS configurations, which significantly improve system reliability [1]. However, achieving near-ideal performance still requires hardware advancements and better channel estimation techniques to reduce phase inaccuracies.

Device-to-Device (D2D) communication is a new paradigm that appears to be a promising component in the 5G. D2D can be defined as a radio communication technology that permits mobile terminals to communicate directly with each other even in a licensed spectrum without the need for base stations(BS). While in a traditional cellular network, all communications must pass through the BS even if both communicating equipments are in range for D2D communication. D2D communication has been considered as a key technology in 5G networks that could achieve higher data rates [20] [21], [22].

D2D communication provides many merits for cellular networks, specifically: (i) high data transmission rate, (ii) energy efficiency enhancement, (iii) extended cellular coverage, (iv) support the overloaded cellular traffic, (v) latency reduction, and (vi) spectral efficiency improvement [23].

D2D communications is a very active topic in research community. Some recent works tackle the problem of power assignment and energy handling in this context of underlaid D2D communications ([24], [25], [26]). The integration of RIS technology in D2D communications offers several compelling advantages that address fundamental challenges in wireless networks. First, RIS can significantly enhance the coverage and reliability of D2D links by creating controllable reflection paths, effectively mitigating blockage issues and reducing outage probability in urban environments. This is particularly crucial for millimeter-wave D2D communications, where line-of-sight paths are often obstructed. Second, RIS enables intelligent interference management by actively shaping the propagation environment, allowing multiple D2D pairs to coexist while maintaining high spectral efficiency. The passive beamforming capabilities of RIS can create focused signal paths between D2D pairs while minimizing interference to neighboring devices [27]. Furthermore, the energy efficiency of D2D communications is substantially improved through RIS deployment, as the passive nature of RIS elements eliminates the need for additional power-hungry RF chains while still providing significant performance gains. The programmable nature of RIS also introduces unprecedented flexibility in network optimization, allowing dynamic adaptation to changing channel conditions and user mobility patterns. Additionally, RIS-aided D2D communications can enhance security by creating favorable channel conditions for intended receivers while degrading potential eavesdropping channels. The cost-effectiveness of RIS implementation, compared to traditional relay systems, makes it an attractive solution for large-scale D2D network deployment, particularly in dense urban scenarios where infrastructure costs are a significant concern [1].

While RIS technology shows promising potential, the optimization of RIS parameters, particularly the number of reflecting elements, remains a critical challenge that directly impacts system performance and implementation costs [1]. Understanding the relationship between the number of RIS elements and key performance metrics such as achievable rate and outage probability is essential for practical deployment considerations [28].

This paper presents a comprehensive analytical framework to optimize RIS configurations in D2D communication scenarios. Specifically, we investigate the fundamental trade-off between the number of RIS elements and system performance metrics, considering both theoretical bounds and practical constraints [3]. Our analysis characterizes how the achievable rate scales with the number of RIS elements while accounting for realistic channel conditions and implementation imperfections [4]. Furthermore, we derive closed-form expressions for outage probability as a function of RIS array size, providing insights into the minimum number of elements required to maintain reliable D2D communications under various channel conditions [5].

The proposed analytical framework addresses several key questions: (i) How does the number of RIS elements affect the achievable rate and outage probability in D2D communications? (ii) What is the optimal number of RIS elements that balances performance gains with implementation complexity? (iii) How do channel conditions and system parameters influence the optimal RIS configuration? Thereafter we present the major contributions of this paper:

- We start by characterizing the channel fading between the D2D sender and the receiver passing through RIS. We express this channel fading as a non-central Chi-squared Distribution. Then we proved through numerical study an approximation of the non-central χ^2 using Gaussian distribution that we define those parameters.
- We express the cumulative density function of the transmit power in general case. A special case of noiseless was derived then.
- We give the expectation of the transmit power in the scenario of noiseless environment.
- We propose a greedy optimization algorithm to determine the number of RIS elements and the phase resolution based on the acceptable overhead duration and quantization penalty. This algorithm presents a lower complexity since no-differentiation is required.

- Finally, we provide numerical and simulation results to show the performance of the proposed approaches. We find that our proposed analytic results match well with simulations results that prove the correctness of our analysis.

The remainder of the paper is as follows; Section II gives the system model used in this work. Section III develops an analysis of the transmit power while guaranteeing a SINR threshold. Section IV gives an algorithm to select the RIS configuration while minimizing the required expectation of the transmit power. Section V gives a numerical analysis. And the last Section concludes the paper.

II. System Model

In an Orthogonal Frequency Division Multiplexing (OFDM) framework, we assume that on each subcarrier only a single pair of D2D users is supported via resource reuse with a cellular user. We consider also that the LOS path between D2D users is blocked or the distance between D2D users is long. So D2D users communicate through an RIS having N passive reflective elements with an intelligent and ideal phase shifts . Then the received signal at UED_D, serves as $D2D$

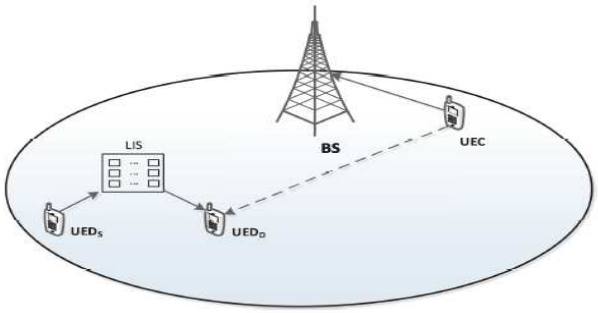


Fig. 1. D2D communication assisted with RIS in a cellular network (based on [29]).

destination, can be expressed as :

$$y_D = \sqrt{P_s}\left[\sum_{i=1}^{N} f_i d_{SR}^{-\alpha/2} e^{j\theta_i} g_i d_{RD}^{-\alpha/2}\right] x_s + \sqrt{P_c} h d_{CD}^{-\alpha/2} x_c + n \tag{1}$$

with $n \sim CN(0, N_0)$ is the additive white gaussian noise(**AWGN**) with variance N_0,P_s is the transmit power of UED_S ($D2D$ source), P_C the transmit power of the cellular user UEC, x_s stands for the UED_S transmit signal with unit energy and x_c for the cellular transmit signal with unit energy. We assume that all links are affected by Rayleigh fading, h is the channel between the cellular user and D2D receiver, and the channels between UED_S and RIS and between RIS and UED_D, are described as follows: $f_i = \tilde{f}_i e^{-j\phi_i}$ and $g_i = \tilde{g}_i e^{-j\varphi_i}$, respectively. With, $\tilde{f}_i$ and $\tilde{g}_i$ are the corresponding channel amplitudes, and ϕ_i and φ_i are the channel phases which are uniformly distributed between $(-\pi, \pi]$. θ_i is the phase shift introduced by the RIS n^{th} element. The above distances d_{SR}, d_{RD} and d_{CD} are between UED_S and RIS, RIS and UED_D, UEC and UED_D, respectively.

So the received SINR at UED_D is :

$$\gamma = \frac{P_s |\sum_{i=1}^{N} \tilde{f}_i \tilde{g}_i e^{j(\theta_i - \phi_i - \varphi i)}|^2 d_{SR}^{-\alpha} d_{RD}^{-\alpha}}{P_c |h|^2 d_{CD}^{-\alpha} + N_0} \tag{2}$$

Under the assumption that the RIS has the full knowledge of the channels phases of f_i and g_i , and the RIS can be smartly configured to fully eliminate the phase shifts by sitting $\theta_i = \angle f_i g_i + \theta_i^{\epsilon}$ where θ_i^{ϵ} the phase error follows uniform distribution between [-π/L, π/L] And we work with BPSK modulation, so $x_s, x_c \in \{-1, 1\}$, hence only the real part of the signal has an impact on the detection performance, so the SINR becomes :

$$\gamma = \frac{P_s (\sum_{i=1}^{N} \tilde{f}_i \tilde{g}_i v_i)^2 d_{SR}^{-\alpha} d_{RD}^{-\alpha}}{P_c |h|^2 d_{CD}^{-\alpha} + N_0} \tag{3}$$

with $v_i = cos(\theta_i^{\epsilon})$ as $\angle f_i g_i = \phi_i + \varphi_i$ and $\tilde{f}_i$, $\tilde{g}_i$ follows Rayleigh distribution with scale parameter $\frac{1}{\sqrt{2}}$.

We consider $I = P_c |h|^2 d_{co}^{-\alpha}$.

III. Performance Analysis

A. Transmit Power CDF of Assisted RIS D2D communication

Let: $A = \sum_{i=1}^{N} \tilde{f}_i \tilde{g}_i v_i$ and $B = A^2$.
According to the central limit theorem (CLT) [30], for a large number of reflecting elements, A converges to a Gaussian distribution. The Literature stats that from $N \geq 30$ [31], [32] the CLT is applicable. That is $A \sim N(\mu_a, \sigma_a^2)$, where μ_a is the mean and σ_a^2 is the variance.

Lemma 1. *The parameters of the distribution of A can be given as follows: $\mu_a = \frac{NL\sin(\pi/L)}{4}$ and*

$$\sigma_a^2 = \frac{NL}{4}\left(\frac{1}{2} - \frac{1}{\pi} arcsin(cos(\frac{2\pi}{L})) + \frac{1}{\pi} sin(\frac{2\pi}{L}) - \frac{L}{4} sin^2(\frac{\pi}{L})\right)$$

The proof of this lemma is given in Appendix A.
As relationships between probability distributions states : B has a non-central chi-square distribution with one degree of freedom $k = 1$ and non centrality parameter $\lambda = \frac{\mu_a^2}{\sigma_a^2}$.
Let $\overline{\gamma} = \frac{\beta (d_{SR} d_{RD})^{\alpha}}{p}$, $I = P_c |h|^2 d_{CD}^{-\alpha}$, $a = \frac{\overline{\gamma} P_c d_{CD}^{-\alpha}}{2\sigma_a^2}$, $b = \frac{\overline{\gamma} N_0}{2\sigma_a^2}$ and $c = \frac{\mu_a}{\sigma_a \sqrt{2}}$.

Theorem 1. *The cumulative density function (CDF) of the transmit power P_s can be expressed as:*

$$\mathbb{P}(P_s \leq p) = 1 - \frac{\text{erf}\left(\sqrt{b} + c\right) + \text{erf}\left(\sqrt{b} - c\right)}{2} - \frac{\sqrt{a}}{2\sqrt{a+1}} \, \mathrm{e}^{\frac{b}{a} - \frac{c^2}{a+1}} \cdot \left[2 - \text{erf}\left(\frac{(a+1)\sqrt{b} + ac}{\sqrt{a(a+1)}}\right) - \text{erf}\left(\frac{(a+1)\sqrt{b} - ac}{\sqrt{a(a+1)}}\right)\right] \tag{4}$$

The error function (also called the Gauss error function), denoted by erf, is a function $\text{erf} : \mathbb{C} \to \mathbb{C}$ *defined as:*

$$\mathbb{P}(P_s \leq p) = 1 - \frac{\operatorname{erf}\left(\sqrt{\frac{\tau}{p}} + c\right) + \operatorname{erf}\left(\sqrt{\frac{\tau}{p}} - c\right)}{2} - \frac{1}{2}\sqrt{\frac{\rho}{\rho+p}}\,\mathrm{e}^{\frac{\tau}{\rho} - \frac{c^2 p}{p+\rho}}\left[2 - \operatorname{erf}\left(\frac{(\rho+p)\sqrt{\frac{\tau}{p}} + c\rho}{\sqrt{\rho(\rho+p)}}\right) - \operatorname{erf}\left(\frac{(\rho+p)\sqrt{\frac{\tau}{p}} - c\rho}{\sqrt{\rho(\rho+p)}}\right)\right] \tag{5}$$

$$\operatorname{erf} z = \frac{2}{\sqrt{\pi}} \int_0^z e^{-t^2}\,\mathrm{d}t.$$

The proof of this theorem is given in the appendix B.
Let appearing the variable p in the Eq. (4). By changing a by $a = \rho/p$ with $\rho = \frac{\beta P_c}{2\sigma_a^2}\left(\frac{d_{SR} d_{RD}}{d_{CD}}\right)^{\alpha}$, and b by $b = \tau/p$ with $\tau = \frac{\beta N_0}{2\sigma_a^2}\left(d_{SR} d_{RD}\right)^{\alpha}$, and c remains the same. So, we get the result in Eq. (5) presented on the top of this page.

In the following, we give another approximation of the transmit power CDF, using the distribution of B.

Proposition 1. *For large RIS elements number, the transmit power CDF can be approximated as:*

$$\mathbb{P}(P_s \leq p) \approx \frac{\mathrm{e}^{\frac{4rs+1}{4r^2}}\left(\operatorname{erf}\left(\frac{2rs+1}{2r}\right) - 1\right) - \operatorname{erf}(s) + 1}{2} \tag{6}$$

where $r = \frac{\overline{\gamma} P_c d_{CD}^{-\alpha}}{\sigma_b\sqrt{2}}$ and $s = \frac{\overline{\gamma} N_0 - \mu_b}{\sigma_b\sqrt{2}}$ and μ_b, σ_b^2 are the Mean and Variance of B, with: $\mu_b = \mu_a^2 + \sigma_a^2$ and $\sigma_b^2 = 2\sigma_a^4 + 4\mu_a^2\sigma_a^2$.

The proof of this proposition is given in Appendix C.

We consider the special situation where the noise can be neglected. The result is given in Proposition 2

Proposition 2. *In noiseless case scenario the transmit power CDF becomes:*

$$\mathbb{P}(P_s \leq p) = 1 - \sqrt{\frac{\rho}{p+\rho}}\mathrm{e}^{-c^2 p/(p+\rho)} \tag{7}$$

The proof of this proposition can obtained by putting τ to 0 in eq. (5), since when $N_0 \to 0$, $b \to 0$, so the proposition is deduced.

B. Transmit Power Expectation

In this subsection, we are interested in analyzing the expectation of the transmit power of the D2D device.

Theorem 2. *Let $\rho = \frac{\beta P_c}{2\sigma_a^2}\left(\frac{d_{SR} d_{RD}}{d_{CD}}\right)^{\alpha}$.*
In the context of noiseless environment, the expectation of the transmit power can be derived as (Eq. 8):

$$\mathbb{E}[P_s] = 2\rho\mathrm{e}^{-c^2}\left(\sqrt{\pi}\,c\operatorname{erfi}(c) - \sqrt{\pi}\,c\operatorname{erfi}\left(c\sqrt{\frac{\rho}{P_{max}+\rho}}\right) - \mathrm{e}^{c^2} + \frac{\mathrm{e}^{\frac{c^2\rho}{P_{max}+\rho}}}{\sqrt{\frac{\rho}{P_{max}+\rho}}}\right) \tag{8}$$

With the imaginary error function $\operatorname{erfi} : \mathbb{C} \to \mathbb{C}$ is defined as $\operatorname{erfi} z = -i \operatorname{erf} iz$, where i is the imaginary unit.

The proof of this theorem is given bellow.

Proof. In the case of noiseless scenario, the CDF of the transmit power is given as: $1 - \sqrt{\rho/(\rho+p)}e^{-pc^2/(p+\rho)}$. Since, the expectation is the integral of $1 - CDF$, we can write:

$$\mathbb{E}[P_s] = \int_0^{P_{max}} \sqrt{\frac{\rho}{p+\rho}}\mathrm{e}^{-c^2 p/(p+\rho)}\,dp \tag{9}$$

By applying the variable replacement $x = p + \rho$, the integral becomes:

$$\mathbb{E}[P_s] = \sqrt{\rho}\mathrm{e}^{-c^2}\int_{\rho}^{P_{max}+\rho} x^{-1/2}\mathrm{e}^{c^2\rho/x}\,dx \tag{10}$$

This concludes the proof.

□

C. Transmit power and Rate trade-off Optimization

Before the data transmission phase begins, it is essential to estimate the channels from the transmitter to the RIS and from the RIS to the receiver, and to configure the optimized phase shifts at the RIS. The evaluation of the rate in the previous subsection does not consider overhead to configure dynamically the RIS.Transmitting the optimized phase matrix to the RIS before data transmission can introduce significant overhead, particularly when N is large. We define T_F as the duration of the feedback phase, which relies on the feedback power and the feedback channel bandwidth. Additionally, T_E is the duration of the channel estimation phase before feedback and communication. The total slot time T, which includes channel estimation, feedback, and data communication phase of duration $T - T_E - T_F$, determines the system's achievable rate and energy efficiency. So the actualized expression is given as (11)

$$R_{in} = \left(1 - \frac{T_E + T_F}{T}\right)\log_2(1 + SINR) \tag{11}$$

Following the model developed in [33], we have:

$$T_E = T_0(N+1)$$

with T_0 the duration of each pilot tone. As for T_F , after resource optimization, the transmitter sends a control signal to the RIS to configure the phase shifts. Denoting by h_F the scalar feedback channel from the RIS to the transmitter, p_F is the power used during the feedback phase and B_F is the bandwidth of the feedback channel, it holds that:

$$T_F = \frac{N b_F}{B_F log(1 + \frac{p_F|h_F|^2}{N_0 B_F})}, \tag{12}$$

with b_F is the number of feedback bits for each reflecting element of the RIS. In this work, we consider that:
$b_F = k.log_2(L)$.

This formulation encapsulates a crucial design challenge in RIS systems. While increasing the number of RIS elements

(N) and (L) can potentially enhance system performance and reduce the overall power consumption P_s , it simultaneously leads to increased overhead in terms of channel estimation time T_E and feedback time T_F. This creates an inherent tension between performance optimization and system overhead, necessitating careful consideration of the trade-off between these competing objectives.

The optimization problem seeks to determine the optimal configuration that minimizes the expected power consumption while ensuring that the total overhead remains within acceptable bounds defined by T_{max}. The joint optimization of N and L must therefore balance the potential benefits of increased RIS elements and L against the associated costs in terms of system overhead and computational complexity.

The fundamental trade-off in RIS-assisted D2D communications can be formulated as an optimization problem:

$$\begin{aligned} &\min_{N,L} \mathbb{E}[(P_s)] \\ &\text{s.t.} \quad T_E + T_F \leq T_{\max} \end{aligned}$$

The **quantization penalty** in RIS refers to the degradation in system performance caused by finite phase resolution in RIS-assisted communication systems. This penalty is defined as the increase in the Bit Error Rate (BER) due to phase quantization, expressed as the ratio of the BER with quantization (P_e) to the BER with infinite phase resolution (P_e^∞). The quantization penalty is given by the formula:

$$\Psi(L) = 10 \log_{10} \left(\frac{P_e}{P_e^\infty} \right)$$

where $\Psi(L)$ represents the penalty in decibels (dB), and P_e and P_e^∞ are the BERs with finite and infinite phase resolution, respectively. This penalty arises because RIS elements can only apply phase shifts with limited precision, which prevents perfect phase alignment at the receiver and reduces the constructive combining of signals. As a result, the BER is higher compared to an ideal RIS with infinite phase resolution. In [19], the authors state that for higher quantization levels ($L \geq 3$), the penalty behaves as

$$\Psi(L) = 10 \log_{10} \left(\frac{L \tan(\pi/L)}{\pi} \right)$$

where increasing L reduces the penalty due to finer phase resolution. As L approaches infinity, the quantization penalty approaches zero, implying that the BER reaches the ideal case. For example, with 2 quantization levels (1-bit), the penalty is severe, but as L increases (e.g., $L = 8$ or $L = 16$), the penalty significantly decreases, improving performance. Thus, while increasing L reduces the penalty, it does not completely eliminate it unless L becomes infinitely large .
Our optimization problem becomes:

$$\begin{aligned} &\min_{N,L} \mathbb{E}[(P_s)] \\ &\text{s.t.} \quad T_E + T_F \leq T_{\max} \\ &\Psi(L) \leq \psi_0 \end{aligned}$$

The optimization problem at hand exhibits several noteworthy characteristics:

- The objective function $\mathbb{E}[(P_s)]$ (expected power consumption) is continuous and differentiable with respect to both N and L. However, N and L are integers.
- The problem includes two inequalities constraint i) $T_E + T_F \leq T_{\max}$ and $\Psi(L) \leq \psi_0$ that are also differentiable.
- The optimization goal is to minimize power consumption while satisfying overhead constraints.

Given these characteristics, the system to optimize is a non-linear integer programming problem. That is, it is classified as NP-hard. Traditionally, such problems have been approached using the Karush-Kuhn-Tucker (KKT) theoretical framework combined with Branch and Bound algorithms. The KKT conditions provide necessary conditions for optimality through the Lagrangian function, while Branch and Bound helps navigate the discrete solution space [34]. However, this classical approach faces significant limitations in our context; the differential of the objective function is challenging, and these approaches often lead to local optima and suffer from high computational complexity, making them impractical for real-time RIS configuration.

To overcome these limitations, we propose a new algorithm based on greedy approach. This novel approach addresses the aforementioned challenges by searching iteratively the best solution profiting of the characteristics of the objective function. Our proposed solution demonstrates superior computational efficiency, making it particularly well-suited for practical RIS deployment scenarios where rapid adaptation to changing network conditions is crucial.

There are also other approaches, like using Deep Learning Constrained Optimization (DL-CO). But, in our model, the DL-CO approach is unnecessarily complex: it relies on gradient-based optimization, which is poorly suited for discrete variables and monotonic objectives, and it is very slow, it needs O(iterations) to compute the optimal values, and it introduces approximation errors due to rounding.

IV. Greedy Algorithm for RIS Configuration

It is clear that to enhance the penalty, L have to be large. The number of RIS elements N is also large. Thus, $\mu_a \approx \frac{N\pi}{4}$ and the variance $\sigma_a^2 \approx \frac{N}{4}\left(2 - \frac{\pi^2}{4}\right)$. It is clear that $T_E + T_F$ is increasing related to N and L. Based on the Proposition 3 and Remark.1, $\mathbb{E}[P_s(N, L)]$ can be considered decreasing with N and slightly decreasing with L.

Proposition 3. *For large values of N, the transmit power expectation decreases as N grows.*

Proof. In the following, we present an analysis of the function:

$$\mathbb{E}[P_s](n) = \sqrt{\rho} \cdot e^{-c^2} \cdot \int_{\rho}^{\rho + P_{max}} x^{-1/2} \cdot \exp\left(\frac{c^2 \rho}{x}\right) dx,$$

For large values of n, $c \propto \sqrt{n}$ and $\rho \propto 1/n$. We can put: $c = k\sqrt{n}$, $\rho = \frac{\gamma}{n}$.

To do this, we will analyze the behavior of $\mathbb{E}[P_s](n)$ as n changes, focusing on the integral and the prefactors.—

Start by rewrite $\mathbb{E}[P_s](n)$ in terms of n by substituting $c = k\sqrt{n}$ and $\rho = \frac{\gamma}{n}$ into $\mathbb{E}[P_s](n)$:

$$\mathbb{E}[P_s](n) = \sqrt{\frac{\gamma}{n}} \cdot \exp(-k^2 n) \cdot \int_{\frac{\gamma}{n}}^{\frac{\gamma}{n}+P} x^{-1/2} \cdot \exp\left(\frac{k^2\gamma}{x}\right) dx.$$

Let analyze the integrand: $x^{-1/2} \cdot \exp\left(\frac{k^2\gamma}{x}\right)$. Since $x^{-1/2}$ decreases as x increases. And $\exp\left(\frac{k^2\gamma}{x}\right)$ decreases as x increases (since $\frac{k^2\gamma}{x}$ decreases).

Thus, the integrand decreases as x increases, and the integral is dominated by the region near the lower limit $x = \frac{\gamma}{n}$.

For large n, the lower limit $\frac{\gamma}{n}$ becomes very small, and the integrand near $x = \frac{\gamma}{n}$ grows very large. However, the integral $I(n)$ is bounded and approaches a constant value as n increases.

Now, we analyze the pre-factors:

$$\sqrt{\frac{\gamma}{n}} \cdot \exp(-k^2 n).$$

The term $\sqrt{\frac{\gamma}{n}}$ decreases as n increases. Also, the term $\exp(-k^2 n)$ decreases exponentially as n increases.

Thus, the pre-factors decay rapidly as n increases.

Combining the results as the integral $I(n)$ is dominated by the region near $x = \frac{\gamma}{n}$ and approaches a constant value for large n. The prefactors $\sqrt{\frac{\gamma}{n}} \cdot \exp(-k^2 n)$ decay rapidly as n increases.

Therefore, $\mathbb{E}[P_s](n)$ is dominated by the decaying prefactors, and it decreases as n increases.

□

Remark 1. *It is worth noting that the impact of L is less important. However, for large values of L, $\mu_a \to N\pi/4$ and $\sigma_a^2 \to N\left(1/2 - \pi^2/16\right)$. So, ρ and c become independent of L. And by the way, $\mathbb{E}[P_s]$ dependents slightly of L.*

Since for large L, the transmit power expectation $\mathbb{E}[P_s]$ depends slightly on L, we can solve the problem firstly related to N, then search the optimal value of L.

$$\begin{aligned} &\min_{N,L} \mathbb{E}[P_s] \\ &\text{s.t.} \quad T_E + T_F \leq T_{\max} \\ &\Psi(L) \leq \psi_0 \end{aligned}$$

For the notation simplification, we denote by the following: $f(n,l) = \mathbb{E}[P_s]$, $g(n,l) = T_E + T_F$, $h(l) = \Psi(L)$

For the resolution of this problem, we propose a greedy algorithm 1. We start with a lower bound for N and L. Knowing that the objective function decreases with N and L, we progressively increment N and we seek the best value for L that guaranties that the constraints still satisfied. The optimal solution will lie at the boundary of the feasible region (i.e., the smallest N and L that satisfy all constraints). So, our algorithm will not fall into local optimums.

Let analyze the time complexity of the algorithm. Denote by: $N_p = n_{\max} - n_{\min} + 1$ and $L_p = l_{\max} - l_{\min} + 1$. The total number of iterations is:$\mathcal{O}(N_p \cdot L_p)$. Each iteration performs: Constraint checks: $g(n,l) \leq T_{\max}$ and $h(l) \leq Q_{\max}$ that is $\mathcal{O}(1)$, and the evaluation of $f(n,l)$ that involves an integral calculation.

Assume the integral is approximated using a quadrature method, such as Gaussian quadrature or Simpson's rule / trapezoidal rule. The complexity is $\mathcal{O}(Q)$ for Q evaluation points for fixed accuracy. So, the cost of computing $f(n,l) = \mathcal{O}(Q) = \mathcal{O}(1)$ (if Q is constant).

Then, the total time complexity of the proposed greedy algorithm is: $\mathcal{O}(N_p \cdot L_p)$

Algorithm 1 Greedy Transmit Power Optimization

Define Functions:
  $\mu_a(n,l)$, $\sigma_a(n,l)$, $c(n,l)$, $f(n,l)$, $T_E(n,l)$, $T_F(n,l)$, $g(n,l)$, $h(l)$
Initialize Parameters:
  $T_{\max} \leftarrow$ Feed back Constraint limit
  $Q_{\max} \leftarrow$ Quantization Constraint limit
  $n_{\min}, n_{\max} \leftarrow$ Valid range for n
  $l_{\min}, l_{\max} \leftarrow$ Valid range for l
  $best_n \leftarrow n_{\min}$
  $best_l \leftarrow l_{\min}$
  $best_value \leftarrow +\infty$ ▷ Initially a very large value
$improved \leftarrow$ false
for $n = n_{\min}$ to $n_{\max}$ **do**
  for $l = l_{\min}$ to $l_{\max}$ **do**
    if $g(n,l) \leq T_{\max}$ and $h(l) \leq Q_{\max}$ **then** ▷ Check both constraints
      $new_value \leftarrow f(n,l)$
      if $new_value < best_value$ **then** ▷ Objective function is decreasing
        $best_n \leftarrow n$
        $best_l \leftarrow l$
        $best_value \leftarrow new_value$
        $improved \leftarrow$ true
      end if
    end if
  end for
end for
Output best solution: $best_n$, $best_l$, $best_value$

V. Numerical and Simulation Results

In this section, we provide numerical and simulation assessment of our propositions to prove there effectiveness.

A. Simulation Parameters

The values used for parameters considered in this work are as follows: $P_c = 20dBm$, $d_{CD} = 120m$, $d_{SR} = 20m$, $d_{RD} = 20m$, $\beta = 20dB$, $N_0 = -100dB$ and $-110dB$. We consider, for values of N, they are taken between 16 and 1100, as stated by [35], [36]. Also, for values of L, they are from 2 to big values [19].

B. Simulation Results

For the first simulation, we evaluate the analytic expression of the cdf of the transmit power as comparison with the

approximated one and the case of noiseless. The evaluation is done for $N = 300$, $L = 20$, the $SINR$ threshold $\beta = 20dB$. The result is given in Fig. 2 and Fig. 3. The results presented show that for dense environment, i.e., the path-loss exponent increases, the transmit power increases. That is, the transmit power is less than a value p_0 decreases, which means that transmit power increases while α increases. This is real since with high path-loss, the transmission power have to be larger to let the receiver required $SINR$ by ensured. Indeed, we can see that the analytic and approximation results are identical with path-loss exponent α. The noiseless scenario matches with analytic and approximation results for lower path-loss exponents i.e., $\alpha = 2$ and $\alpha = 3$. However, in the case of harsh environments, with high path-loss exponent (here $\alpha = 4$), the noiseless presents low transmit power than analytic ans approximation expressions. This is due to the fact that if α is important, the impact of the transmit power of the interferer becomes in the same or even less than the noise. Which means, that the noise in the denominator of the expression of the $SINR$ given in Eq. (3) cannot be negligible as compared to the first term in $P_c|h|^2 d_{CD}^{-\alpha} + N_0$. As a result, the cdf of the transmit power can be approximated reliably by the Eq. (7) in the case of α is not high and the power of noise N_0 is low as we can see in Fig. 3 for $\alpha = 4$.

Fig.4 depicts the cdf of the transmit power for $SINR$ $\beta = 20dB$ of the required $SINR$. $N = 300$, $L = 20$. The transmit power is constrained by its maximum value to $23dBm$. The noise power is set to $N_0 = -110dB$. As we can observe, the analytical results given in Eq. (5) match better with simulations ones. That prove the effectiveness of our analysis.

In the next simulation, we consider a path-loss exponent $\alpha = 2$. The rest of parameters are the same as the previous simulation. Fig.5 gives the expectation of the transmit power for different values of L and N. As we can see, This expectation deceases as N or L increase. We observe also that for low values of N, the simulation values are slightly over the analytic ones. This is due a condition required by the CLT. Additionally, we can observe that the impact of increasing L becomes effective-less as L grows; the impact on the expectation of the transmit power is relatively important for $L = 4$ than $L = 20$ or $L = 40$ where the curves become superposed.

The following experiment is dedicated to the assessment of the expectation of the transmit power. The simulation parameters for this experiment are as follows: The pilot duration is equal to $100\mu s$, the Feedback channel bandwidth is set to $B_F = 10MHz$, the Feedback transmit power is $p_F = 0.1W$, the feedback channel power $h_F^2 = 0.1$. The maximum duration of feedback and estimation $T_{max} \in \{0.1ms, 0.2ms, 0.3ms\}$. The maximum transmit power $P_{max} = 23dBm$. And the Feed back message length $k = 1.5$ of bits used to code L i.e., $log_2(L)$ that is the payload of the packet [1], meaning that an extra bits control

[1]The feedback is protocol dependent. Exta bits are used to form the feedback packet. For a half of the bits length coding L for packet control still acceptable for large L. However, for L coded by a short number of bits, the packet control can have a length surpassing L bits coding. Reader can find extensive details in the case of Internet Protocol in [37]

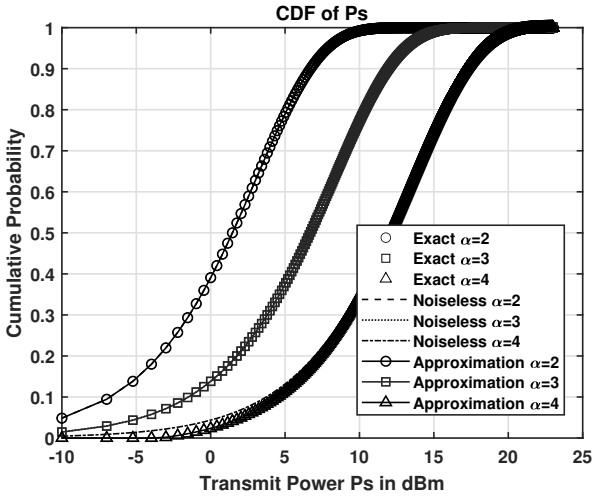


Fig. 2. Transmit Power CDF Comparison Analytic vs Approximation vs Noiseless $N_0 = -110dB$.

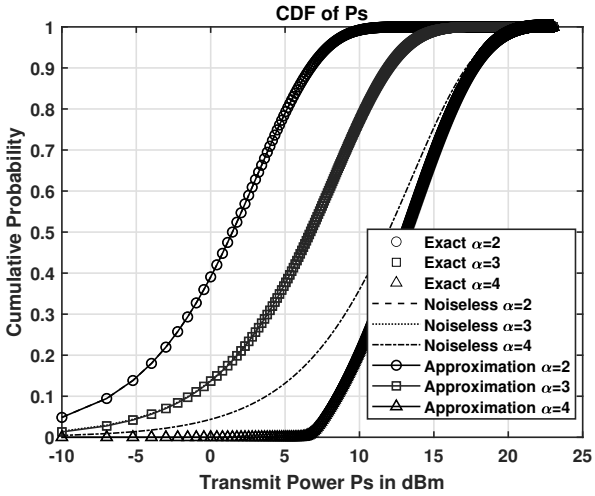


Fig. 3. Transmit Power CDF Comparison Analytic vs Approximation vs Noiseless $N_0 = 100dB$.

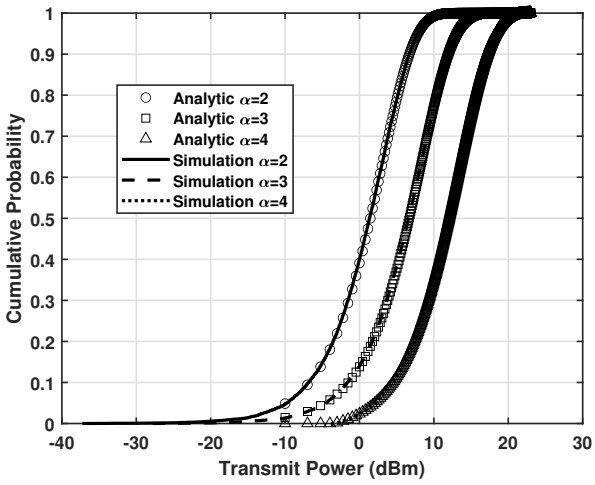


Fig. 4. Comparison between analytical and simulation Transmit Power CDF for different α

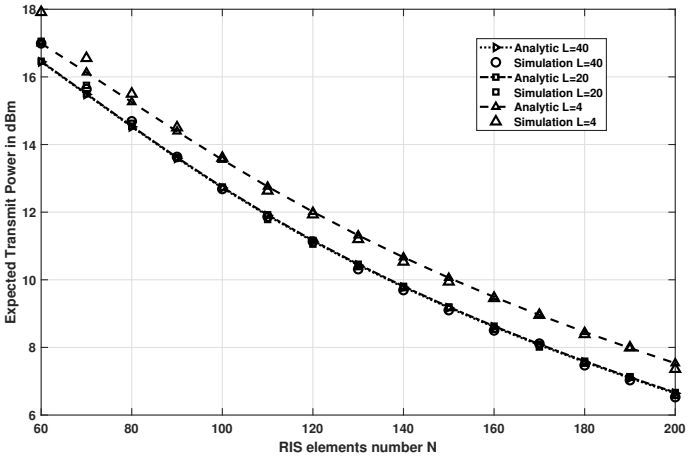


Fig. 5. Transmit Power Expectation vs N and L

are used for the message of the feedback for transmitting the information on the phase quantization. In Table I, we can see

Constrained $T_{max}(ms)$	0.1	0.2	0.3
$N_{Optimal}$	378	757	1136
$L_{Optimal}$	58	58	58
Optimal $\mathbb{E}[P_s]$ (dBm)	1.0602	-4.9971	-8.5310
$T_E + T_F$ (ms)	$9.9802.10^{-2}$	$1.9986.10^{-1}$	$2.9991.10^{-1}$
Effective Penalty	1.001	1.001	1.001

TABLE I
EFFECT OF THE T_{max} PARAMETER.

the impact of T_{max} limitation on the RIS parameters selection and then on expectation of the transmit power. When T_{max} increases, we have more relaxation on the first constraint permitting to choose large values on N and then decreasing the transmit power. Since, the impact of N is important on the power expectation than L, we observe that the value of L still constant.

In the case where the constraint on the quantization penalty,

Constrained Ψ	1.00001	1.0001	1.01
$N_{Optimal}$	245	298	514
$L_{Optimal}$	580	182	19
Optimal $\mathbb{E}[P_s]$ (dBm)	-5.1497	-6.8645	-1.5874
$T_E + T_F$ (ms)	$9.9979.10^{-2}$	10^{-1}	$9.9823.10^{-2}$
Effective Penalty	1.0000	1.0001	1.0092

TABLE II
EFFECT OF THE Ψ PARAMETER.

we observe that L decreases with Ψ increasing since this penalty linked directly to L(see Table II).

In the last experiment, we investigate the evolution of the transmit power when the distance of the interferer to the receiver increases for different value of the required $SINR$ threshold β. In the simulation parameter $\alpha = 3$. We consider $N = 378$ and $L = 58$. As depicted in this figure, the expected transmit power decreases as the interferer is so far from the receiver. This is explained by the fac that when d_{CD} becomes large, the impact of the transmit power of the interferer on the receiver decreases as the effect of the path becomes important. When the required $SINR$ is high, the required expected transmit power of the D2D sender must increase to guarantee this requirement. Indeed, we can observe that theoretical and simulation results are very near and become identical for large distance or when β decreases.

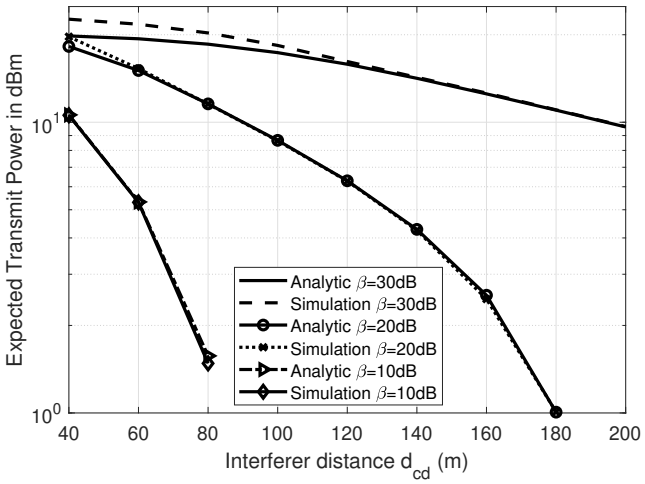


Fig. 6. Transmit Power Expectation vs Interferer distance to the D2D receiver.

VI. CONCLUSION

In this paper we considered a RIS assisted D2D communications using uplink frequency band. A cellular user is considered as interferer. We considered an RIS composed of N elements and giving a discrete phase configuration, i.e., a phase error in $[-\pi/L, \pi/L]$. We derived the channels fading from D2D sender to its receiver. Then we gave the expression of the $SINR$ at the receiver. We analyzed the distribution of the transmit power of the D2D transmitter to meet a required SINR. Then, we express the expectation of the transmit power. Based on this expectation, we proposed an optimization algorithm to determine the configuration of RIS, i.e., the number of elements N and the phase resolution L to minimize the transmission power while guaranteeing an acceptable overhead duration with respect to quantization levels. The simulations results prove the effectiveness of the analytic studies.

APPENDIX A

Proof of the Lemma 1.

Proof. Let: $z_i = |\tilde{f}_i||\tilde{g}_i|v_i$. Based on [19], the pdf of z_i is given by:

$$f_{z_i}(z) = L.e^{-2z} - \frac{2L}{\pi}\int_0^{\pi/2} e^{-2z\sqrt{1+(\frac{tg\pi/L}{sin\phi})^2}}\, d\phi \qquad (13)$$

We can compute the expectation of z_i (denoted as μ_{z_i}) as follows:

$$\begin{aligned}\mathbb{E}[z_i] &= \int_0^\infty z.f_{z_i}(z)\,dz \\ &= \int_0^\infty z\left(L.e^{-2z} - \frac{2L}{\pi}\int_0^{\pi/2} e^{-2z\sqrt{1+(\frac{tg\pi/L}{sin\phi})^2}}\,d\phi\right)dz \\ &= \frac{L}{4}sin(\pi/L)\end{aligned} \tag{14}$$

The variation $\sigma_{z_i}^2$ of z_i can be expressed as:

$$\sigma_{z_i}^2 = \int_0^\infty z^2.f_{z_i}(z)\,dz - \mu_{z_i}^2 \tag{15}$$

Replacing the pdf of z_i, we have:

$$\sigma_{z_i}^2 = \int_0^\infty z^2\left(L.e^{-2z} - \frac{2L}{\pi}\int_0^{\pi/2} e^{-2z\sqrt{1+(\frac{tg\pi/L}{sin\phi})^2}}\,d\phi\right)dz - \mu_{z_i}^2 \tag{16}$$

Let

$$I = L.\int_0^\infty z^2e^{-2z}dz$$

and

$$J = -\frac{2L}{\pi}\int_0^\infty\int_0^{\pi/2} z^2e^{-2z\sqrt{1+(\frac{tg\pi/L}{sin\phi})^2}}\,d\phi\,dz$$

.

Using integration by parts, we obtain $I = L/4$.

For the integral J, the two integrations are convergent and the variables are independent. So we can interchange those integrals and we can rewrite

$$J = -\frac{2L}{\pi}\int_0^{\pi/2}\int_0^\infty z^2e^{-2z\sqrt{1+(\frac{tg\pi/L}{sin\phi})^2}}\,dz\,d\phi$$

Handling then this integral:

$$\begin{aligned}J_1 &= \int_0^\infty z^2e^{-2z\sqrt{1+(\frac{tg\pi/L}{sin\phi})^2}}\,dz \\ &= \frac{1}{4}\left(1+(\frac{tg(\pi/L)}{sin(\phi)})^2\right)^{-3/2}\end{aligned} \tag{17}$$

Now, we calculate the integral

$$J_2 = \frac{1}{4}\int_0^{\pi/2}\left(1+(\frac{tg(\pi/L)}{sin(\phi)})^2\right)^{-3/2}\,d\phi$$

Doing the variables change, $x = sin(\phi)$, J_2 becomes:

$$\begin{aligned}J_2 &= \frac{1}{4}\int_0^1 \frac{x^3}{\sqrt{1-x^2}(x^2+tg(\pi/L)^2)^{\frac{3}{2}}}\,dx \\ &= -\frac{\left(2u^2+2\right)\arcsin\left(\frac{u^2-1}{u^2+1}\right) - \pi u^2 + 4u - \pi}{4(4u^2+4)}\end{aligned} \tag{18}$$

where $u = tan(\pi/L)$. Knowing that $tan(x)^2+1 = 1/cos(x)^2$, J_2 can be rewritten as:

$$J_2 = -\frac{1}{16}\left(2arcsin(-cos(\frac{2\pi}{L})) - \pi + 2sin(2\pi/L)\right) \tag{19}$$

And J is solved as:

$$J = \frac{L}{4\pi}\left[sin(2\pi/L) - sin^{-1}(cos(2\pi/L)) - \pi/2\right] \tag{20}$$

Then we obtain the following result:

$$\sigma_{z_i}^2 = \frac{L}{4} + \frac{L}{4\pi}\left[sin(\frac{2\pi}{L}) - sin^{-1}(cos(\frac{2\pi}{L})) - \frac{\pi}{2}\right] - \mu_{z_i}^2 \tag{21}$$

Since A is sum of N independent variables, using Central limit theorem for large N, A follows a Gaussian distribution with $\mu_a = N\mathbb{E}[z_i]$ and $\sigma_a^2 = N\sigma_{z_i}^2$. □

APPENDIX B

Proof. Let β be the $SINR$ threshold. Based on Eq. (3), we have:

$$\begin{aligned}\mathbb{P}(P_s \le p) &= \mathbb{P}(B \ge \frac{\beta(d_{SR}d_{RD})^\alpha(I+N_0)}{p}) \\ &= \mathbb{E}_I\left[\,\mathbb{P}(B \ge \overline{\gamma}(I+N_0) \mid I)\right]\end{aligned} \tag{22}$$

To compute $P(B \ge x)$, where $B = A^2$ and $A \sim N(\mu_a, \sigma_a^2)$, we can use the relationship between B and A.

Step 1: Express $P(B \ge x)$ in Terms of A Since $B = A^2$, the event $B \ge x$ is equivalent to:

$$B \ge x \iff A^2 \ge x \iff A \le -\sqrt{x} \text{ or } A \ge \sqrt{x}.$$

Thus: $P(B \ge x) = P(A \le -\sqrt{x}) + P(A \ge \sqrt{x})$.

Since $A \sim N(\mu_a, \sigma_a^2)$, we can express the probabilities using the standard normal CDF Φ: $P(A \le -\sqrt{x}) = \Phi\left(\frac{-\sqrt{x}-\mu_a}{\sigma_a}\right)$, and $P(A \ge \sqrt{x}) = 1 - \Phi\left(\frac{\sqrt{x}-\mu}{\sigma}\right)$.

Therefore: $P(B \ge x) = \Phi\left(\frac{-\sqrt{x}-\mu_a}{\sigma_a}\right) + 1 - \Phi\left(\frac{\sqrt{x}-\mu_a}{\sigma_a}\right)$.

Based on this result,we can rewrite Eq. (22) as:

$$\begin{aligned}\mathbb{P}(P_s \le p) = \mathbb{E}_I\Bigg[\,&\Phi\left(\frac{-\sqrt{\overline{\gamma}(I+N_0)}-\mu_a}{\sigma_a}\right) + \\ &1 - \Phi\left(\frac{\sqrt{\overline{\gamma}(I+N_0)}-\mu_a}{\sigma_a}\right)\Bigg]\end{aligned} \tag{23}$$

We can rewrite this using erf function as:

$$\begin{aligned}\mathbb{P}(P_s \le p) = \mathbb{E}_I\Bigg[\,&1 + \frac{1}{2}\left(\mathrm{erf}\left(\frac{-\sqrt{\overline{\gamma}(I+N_0)}-\mu_a}{\sigma_a\sqrt{2}}\right) - \right. \\ &\left.\mathrm{erf}\left(\frac{\sqrt{\overline{\gamma}(I+N_0)}-\mu_a}{\sigma_a\sqrt{2}}\right)\right)\Bigg]\end{aligned} \tag{24}$$

Let $a = \frac{\overline{\gamma}P_c d_{CD}^{-\alpha}}{2\sigma_a^2}$, $b = \frac{\overline{\gamma}N_0}{2\sigma_a^2}$ and $c = \frac{\mu_a}{\sigma_a\sqrt{2}}$. Note that the h follows Rayleigh distribution with scale parameter $\frac{1}{\sqrt{2}}$, which means that h^2 follows the exponential distribution with scale parameter $2(\frac{1}{\sqrt{2}})^2 = 1$.

The cumulative density function is given as:

$$\mathbb{P}(P_s \le p) = \int_0^\infty\left[1 - \frac{\mathrm{erf}\left(\sqrt{ax+b}+c\right) + \mathrm{erf}\left(\sqrt{ax+b}-c\right)}{2}\right]e^{-x}\,dx \tag{25}$$

Calculating the integral,we got Eq. (26).

And finally, we obtain the result given in Eq. (27), that concludes the proof.

□

$$\mathbb{P}(P_s \leq p) = \left[\frac{\left(\operatorname{erf}\left(\sqrt{ax+b}+c\right) + \operatorname{erf}\left(\sqrt{ax+b}-c\right)\right)}{2\mathrm{e}^{x}} - \frac{\sqrt{a}\,\mathrm{e}^{\frac{b}{a}-\frac{c^2}{a+1}}\left(\operatorname{erf}\left(\frac{(a+1)\sqrt{ax+b}+ac}{\sqrt{a(a+1)}}\right) + \operatorname{erf}\left(\frac{(a+1)\sqrt{ax+b}-ac}{a\sqrt{(a+1)}}\right)\right)}{2\sqrt{a+1}} - e^{-x} \right]_0^{\infty} \tag{26}$$

$$\mathbb{P}(P_s \leq p) = \left[1 - \frac{\left(\operatorname{erf}\left(\sqrt{b}+c\right) + \operatorname{erf}\left(\sqrt{b}-c\right)\right)}{2} - \frac{\sqrt{a}\,\mathrm{e}^{\frac{b}{a}-\frac{c^2}{a+1}}\left(2 - \operatorname{erf}\left(\frac{(a+1)\sqrt{b}+ac}{\sqrt{a(a+1)}}\right) - \operatorname{erf}\left(\frac{(a+1)\sqrt{b}-ac}{a\sqrt{(a+1)}}\right)\right)}{2\sqrt{a+1}} \right] \tag{27}$$

APPENDIX C

Proof. The random variable $B = A^2$, where $A \sim \mathcal{N}(\mu_a, \sigma_a^2)$, follows a non-central chi-squared distribution with 1 degree of freedom. While this distribution is not normal, it can be approximated by a normal distribution under certain conditions:

1) The non-centrality parameter λ is large: The non-centrality parameter is $\lambda = \left(\frac{\mu_a}{\sigma_a}\right)^2$. and When λ is large (i.e., μ_a is large relative to σ_a), the distribution of B becomes more symmetric and bell-shaped, resembling a normal distribution. In our situation $\lambda \propto N$. Then the condition holds.
2) The mean μ_a is large relative to the standard deviation σ_a: If $\mu_a \gg \sigma_a$, the contribution of the central part of the distribution (near $A = 0$) becomes negligible, and the distribution of B is dominated by the squared term A^2, which behaves more like a normal distribution. Since $\frac{\mu_a}{\sigma_a} \propto \sqrt{N}$. Therefore, for large N, This ratio becomes large. Then this condition is satisfied.

The above conditions are satisfied, and $B = A^2$ can be approximated by a normal distribution $B \approx \mathcal{N}(\mu_B, \sigma_B^2)$ with:

- Mean: $\mu_B = \mathbb{E}[B] = \mu_a^2 + \sigma_a^2$.
- Variance:$\sigma_B^2 = \mathrm{Var}(B) = 2\sigma_a^4 + 4\mu_a^2\sigma_a^2$.

Since we proved that B can be approximated using a normal distribution, we can rewrite the transmit power cdf as follows:

$$\begin{aligned} \mathbb{P}(P_s \leq p) &= \mathbb{P}(B \geq \frac{\beta(d_{SR}d_{RD})^{\alpha}(I+N_0)}{p}) \\ &= \mathbb{E}_I\left[\, \mathbb{P}(B \geq \overline{\gamma}(I+N_0) \mid I)\right] \\ &= \mathbb{E}_I\left[\, 1 - \Phi\left(\frac{\overline{\gamma}(I+N_0)-\mu_b}{\sigma_b}\right)\right] \end{aligned} \tag{28}$$

Knowing that $\Phi\left(\frac{x-\mu}{\sigma}\right) = \frac{1}{2}\left[1 + \operatorname{erf}\left(\frac{x-\mu}{\sigma\sqrt{2}}\right)\right]$, rewriting the previous equation as:

$$\begin{aligned} \mathbb{P}(P_s \leq p) &= \frac{1}{2}\int_0^{\infty} \left(1 - \operatorname{erf}(rx+s)\right) e^{-x}\, dx \\ &= \frac{\mathrm{e}^{\frac{4rs+1}{4r^2}}\left(\operatorname{erf}\left(\frac{2rs+1}{2r}\right) - 1\right) - \operatorname{erf}(s) + 1}{2} \end{aligned} \tag{29}$$

That gives the result in the proposition. □

REFERENCES

[1] Q. Wu and R. Zhang, "Towards Smart and Reconfigurable Environment: Intelligent Reflecting Surface Aided Wireless Network," IEEE Communications Magazine, vol. 58, no. 1, pp. 106-112, 2020.

[2] M. Di Renzo et al., "Smart Radio Environments Empowered by Reconfigurable Intelligent Surfaces: How It Works, State of Research, and The Road Ahead," IEEE Journal on Selected Areas in Communications, vol. 38, no. 11, pp. 2450-2525, 2020.

[3] E. Basar et al., "Wireless Communications Through Reconfigurable Intelligent Surfaces," IEEE Access, vol. 7, pp. 116753-116773, 2019.

[4] C. Huang et al., "Holographic MIMO Surfaces for 6G Wireless Networks: Opportunities, Challenges, and Trends," IEEE Wireless Communications, vol. 27, no. 5, pp. 118-125, 2020.

[5] Q. Wu et al., "Intelligent Reflecting Surface Aided Wireless Communications: A Tutorial," IEEE Transactions on Communications, vol. 69, no. 5, pp. 3313-3351, 2021.

[6] M. Abualhayja'a, M. Wagih, A. Centeno, M. A. Imran and L. Mohjazi, "How Much Power Is Needed for RIS to Beat Relays? A Sustainability Framework," in IEEE Access, vol. 13, pp. 64061-64075, 2025, doi: 10.1109/ACCESS.2025.3560131.

[7] Q. Wu and R. Zhang, "Intelligent Reflecting Surface Enhanced Wireless Network via Joint Active and Passive Beamforming," IEEE Trans. Wireless Commun., vol. 18, no. 11, pp. 5394–5409, Nov. 2019, doi: 10.1109/TWC.2019.2936025.

[8] S. Gong et al., "Toward Smart Wireless Communications via Intelligent Reflecting Surfaces: A Contemporary Survey," IEEE Communications Surveys & Tutorials, vol. 22, no. 4, pp. 2283-2314, 2020.

[9] N. Rajatheva et al., "White Paper on Broadband Connectivity in 6G," arXiv preprint arXiv:2004.14247, 2020.

[10] Liu, Yuanwei, et al. "Reconfigurable intelligent surfaces: Principles and opportunities." IEEE communications surveys & tutorials 23.3 (2021): 1546-1577.

[11] Di Renzo, Marco, Fadil H. Danufane, and Sergei Tretyakov. "Communication models for reconfigurable intelligent surfaces: From surface electromagnetics to wireless networks optimization." Proceedings of the IEEE 110.9 (2022): 1164-1209.

[12] Basar, Ertugrul, and H. Vincent Poor. "Present and future of reconfigurable intelligent surface-empowered communications [perspectives]." IEEE Signal Processing Magazine 38.6 (2021): 146-152.

[13] Chongwen Huang; Alessio Zappone; George C. Alexandropoulos; Mérouane Debbah; Chau Yuen. "Reconfigurable Intelligent Surfaces for Energy Efficiency in Wireless Communication," IEEE Transactions on Communications(Volume: 18, Issue: 8, August 2019).

[14] Tang, W., et al. (2021). "Wireless Communications with Reconfigurable Intelligent Surface: Path Loss Modeling and Experimental Measurement," IEEE Transactions on Wireless Communications.

[15] Liu, Y., et al. (2021). "Reconfigurable Intelligent Surface Aided NOMA: A New Frontier for 6G Networks," IEEE Journal on Selected Topics in Signal Processing.

[16] Q. Wu and R. Zhang, "Beamforming optimization for wireless network aided by intelligent reflecting surface with discrete phase shifts," IEEE Trans. Commun., vol. 68, no. 3, pp. 1838-1851, 2020.

[17] S. Abeywickrama, R. Zhang, Q. Wu, and C. Yuen, "Intelligent reflecting surface: Practical phase shift model and beamforming optimization," IEEE Trans. Commun., vol. 68, no. 3, pp. 5849-5863, 2020.

[18] Xu, P., Chen, G., Yang, Z., Di Renzo, M. (2021). Reconfigurable intelligent surfaces assisted communications with discrete phase shifts:

How many quantization levels are required to achieve full diversity? IEEE Wireless Communications Letters, 10(2), 352-368.

[19] I. Trigui, E. K. Agbogla, M. Benjillali, W. Ajib and W. -P. Zhu, "Bit Error Rate Analysis for Reconfigurable Intelligent Surfaces With Phase Errors," in IEEE Communications Letters, vol. 25, no. 7, pp. 2176-2180, July 2021, doi: 10.1109/LCOMM.2021.3071433.

[20] Gismalla, Mohammed Salih Mohammed, et al. "Survey on device to device (D2D) communication for 5GB/6G networks: Concept, applications, challenges, and future directions." IEEE Access 10 (2022): 30792-30821.

[21] Areqi, Manal A., Ammar T. Zahary, and Mansoor N. Ali. "State-of-the-art device-to-device communication solutions." IEEE Access 11 (2023): 46734-46764.

[22] Patil, Priyanka, and Vaibhav Hendre. "Comprehensive Survey on Device-to-Device Communication for Next-Generation Cellular Technology." Future Trends in 5G and 6G (2021): 63-80.

[23] Udit Narayana Kar, Debarshi Kumar Sanyal, "An overview of device-to-device communication in cellular networks," ICT Express, Volume 4, Issue 4, 2018, Pages 203-208, ISSN 2405-9595, https://doi.org/10.1016/j.icte.2017.08.002.

[24] Chinbou, A., Boumaalif, A. & Zytoune, O. D2D Lifetime Analysis in Context of Radio Frequency Energy Harvesting. Wireless Pers Commun 139, 1735–1748 (2024). https://doi.org/10.1007/s11277-024-11692-1

[25] A. Boumaalif and O. Zytoune, "Power Distribution of Device-to-Device Communications Under Nakagami Fading Channel," in IEEE Transactions on Mobile Computing, vol. 21, no. 6, pp. 2158-2167, 1 June 2022, doi: 10.1109/TMC.2020.3035543

[26] Boumaalif A, Zytoune O, El Fadil H, Saadane R. Power Distribution of D2D Communications in Case of Energy Harvesting Capability over $\kappa-\mu$ Shadowed Fading Conditions. Journal of Sensor and Actuator Networks. 2023; 12(1):16. https://doi.org/10.3390/jsan12010016

[27] M. Di Renzo et al., "Smart Radio Environments Empowered by AI Reconfigurable Meta-Surfaces: An Idea Whose Time Has Come," EURASIP Journal on Wireless Communications and Networking, vol. 2019, no. 1, pp. 1-20, 2019.

[28] E. Björnson and L. Sanguinetti, "Power Scaling Laws and Near-Field Behaviors of Massive MIMO and Intelligent Reflecting Surfaces," IEEE Open Journal of the Communications Society, 2021.

[29] Y. Ni, Y. Liu, J. Wang, Q. Wang, H. Zhao and H. Zhu, "Performance Analysis for RIS-Assisted D2D Communication Under Nakagami-m Fading," in IEEE Transactions on Vehicular Technology, vol. 70, no. 6, pp. 5865-5879, June 2021, doi: 10.1109/TVT.2021.3077805.

[30] Le Cam, Lucien. "The central limit theorem around 1935." Statistical science (1986): 78-91.

[31] Q. Wu, R. Zhang, "Intelligent Reflecting Surface-Assisted Wireless Communications: Modeling, Analysis, and Optimization", IEEE Transactions on Wireless Communications, 2020.

[32] E. Björnson, Ö. Özdogan, E. Basar, "Reconfigurable Intelligent Surfaces: A Signal Processing Perspective With Wireless Applications", IEEE Signal Processing Magazine, 2022.

[33] A. Zappone, M. Di Renzo, F. Shams, X. Qian and M. Debbah, "Overhead-Aware Design of Reconfigurable Intelligent Surfaces in Smart Radio Environments," in IEEE Transactions on Wireless Communications, vol. 20, no. 1, pp. 126-141, Jan. 2021, doi: 10.1109/TWC.2020.3023578.

[34] Ronald L. Rardin, "Optimization in operations research", Prentice Hall, (1998).

[35] Zhang, X., et al. (2023). Impact of the Number of Elements and Transmit Power in the Performance of Reconfigurable Intelligent Surface Systems. Proceedings of the 2023 11th International Conference on Computer and Communications Management.

[36] Pei, X., Yin, H., Tan, L., Cao, L., Li, Z., Wang, K., Zhang, K., & Björnson, E. (2021). RIS-Aided Wireless Communications: Prototyping, Adaptive Beamforming, and Indoor/Outdoor Field Trials. arXiv preprint arXiv:2103.00534

[37] Stallings, William. Computer networking with Internet protocols and technology. Upper Saddle River, NJ, USA: Pearson/Prentice Hall, 2004.